An Approach to Predict Galvanic Corrosion Using Identical Couple Electrodes; Investigation of Weld Zone and Parent Alloy in AA6xxx Welded through FSW Technique

M. Amini[*,1], F. Kazemzade, M.H. Moayed and M. Haddad-Sabzevar

Department of Materials and Metallurgical Engineering, Ferdowsi University of Mashhad, P.O. Box 91775-1111, Iran

Abstract: The technology requires fabrication, utilization, maintenance and repairing of structures, causing different materials contact each other in operational environments. Therefore, galvanic corrosion has a great significance. The present work is an approach to investigate the occurrence of galvanic corrosion by applying identical couple electrodes. In this work, an AA6xxx specimen was welded by FSW method. The parent alloy and the weld zone were investigated by various electrochemical examinations including potentiodynamic, potentiostatic and corrosion potential monitoring in 3.5% NaCl solution at room temperature. The results revealed no significant difference in corrosion behavior of WZ and PA. Further investigations on the occurrence of galvanic corrosion carried out over nonidentical and also identical couple electrodes from WZ and PA using ZRA technique. The comparison of mean couple current density showed that the amount in PA/WZ was approximately twice PA/PA and five times WZ/WZ indicating the occurrence of galvanic corrosion between WZ and PA.

Keywords: aluminum alloy; galvanic corrosion; friction stir welding; identical couple electrodes; nonidentical couple electrodes

Introduction

Al–Mg–Si alloys are widely employed in welded fabrications. The inherent corrosion resistance of these alloys is excellent and, individually, they are all suitable for marine services [1]. The welding procedure strongly alters the microstructure by heat-treatment, producing local variations in material composition and structure. These changes increase the dissimilarity of the base metal/welded metal pair causing galvanic corrosion [2,3].

Friction stir welding (FSW) is a solid-state joining process which was patented in 1991 by the Welding Institute in the United Kingdom. The advantages of this process include reduced defects and low residual stresses compared to the conventional fusion welding techniques [4]. The FSW involves an inconsumable, cylindrical and rotating tool (usually hardened steel) which moves between the seam of two butted plates and stirs them together [5].

The FSW of age-hardenable aluminum alloys such as 2xxx, 6xxx, and 7xxx alloys produces a recrystallized weld zone [5] that consists of a nugget, or the stirred zone, the thermo-mechanically affected zone (TMAZ), and a heat affected zone (HAZ) [3].

The corrosion of aluminum alloy friction stir welds is commonly investigated using methods such as immersion tests, polarization techniques, an agar gel exposure, the droplet cell method or cyclic spray tests [6]. A number of studies [3,5,7-11] have been reported in the literature that investigated the corrosion behavior of FSW welded aluminum alloys, but none of these focused on the galvanic corrosion in friction stir weldments.

However, Liu et al. [4] investigated the occurrence of galvanic corrosion in dissimilar friction stir welded joints of AZ31 magnesium alloy and AA 2024 aluminum alloy in two different polishing solutions. The location of corrosion attack was observed in the narrow regions of AZ31 Mg alloy adjacent to AA 2024 regions in the stir zone. The occurrence of galvanic corrosion was due to the formation of Mg/Al galvanic couples with a small ratio of anode-to-cathode surface area. Mujibur Rahaman et al. [1], also, studied the galvanic corrosion of laser weldments of AA6061 aluminum alloy in 3.5% NaCl solution at the room temperature. The weld fusion zone is found to be the most cathodic region of the weldment while the base material is the most anodic region.

Moreover galvanic corrosion has never been investigated using identical couple electrodes, so we present a new method to predict galvanic corrosion. The aim of this research is to investigate the occurrence of galvanic corrosion in weld zone and parent alloy of the friction stir welded joint of 6xxx series aluminum alloy by setting up the identical couple electrodes as well as the nonidentical couple electrodes.

Experimental Procedure

The 7.5 mm thickness plates of aluminum alloy 6xxx series (Al-1.18Mg-0.34Si) were friction stir welded at a travel speed of 300 mm.min^{-1} and the rotation speed of

600 rpm. The shoulder diameter was approximately three times the pin diameter which equals the plate thickness.

Metallographic investigations were carried out on cross section of weld that were wet abraded using a grit number sequence of 400, 600, 800 and 1200, then was polished (1 μm) and etched by boiling HNO_3 (25%) solution. Microstructure examinations were performed using an optical microscope (Olympus Model BX60M) which was linked to a digital camera (JVC Model TK‑C1380).

For electrochemical measurements, specimens were cut into blocks with dimensions up to 10 mm. Then the surfaces of the specimens were ground with silicon carbide sandpaper p320 (in order to make it possible measuring the dimensions and the surface area) and have been embedded in cold-setting resins so to expose only a single surface to the aggressive solution. Then they have been electrically connected with a copper wire, set in a polyethylene tube (also embedded in resin). After that, the specimen surfaces were ground with silicon carbide sandpaper up to No. 600 and finally rinsed with distilled water.

Identical surface area of the parent alloy and the weld zone were selected as working electrodes (is named respectively PA and WZ hereafter) and three types of electrochemical tests have been carried out in 3.5 Wt.% NaCl aqueous solution at room temperature including corrosion potential monitoring, measurements under potential imposition (polarization curves) and open circuit measurements (zero-resistance ammeter, ZRA). The hardware includes a potentiostat, a personal computer and the ectrochemical cell. Data have been obtained using a potentiostat ACM Instruments Model GillAC. For each test, except the potentiostatic polarization, just after immersion the potential is allowed to be stabilized until the variations of voltage become limited to a 3 mV range in 1 min period. Then the tests were started. In order to probing the reproducibility of tests in all cases, they have been repeated and the results presented in the paper are one of the most representative obtained curves.

In order to access the corrosion potential of PA and WZ, corrosion potential monitoring tests were performed in the weld zone as well as in the parent alloy. During the immersion test (1 h), the corrosion potentials of the samples were continuously (every 1 s) measured using a saturated calomel electrode (SCE).

Polarization tests were carried out through the classical three electrode cell technique. The working electrode was the test sample, while the auxiliary electrode was a platinum wire and the reference electrode was a SCE. To obtain the polarization behaviour of PA and WZ and comparing them, polarization test was carried out in the cathodic and anodic directions from the corrosion potential. The investigated potential range was −600 to +600 mV versus the rest potential with a scan rate of 1 mV/s. Potentiostatic tests were also performed at the fixed potentials of 100, 150 and 250 mV on the direction of cathodic and anodic potential versus the corrosion potential of weld zone as well as parent alloy during 1200 s.

Using the open circuit measurement technique, the galvanic current density (i_G) and the galvanic potential (E_G) precisely measured between identical surface area and nonidentical (in order to avoid the effect of the
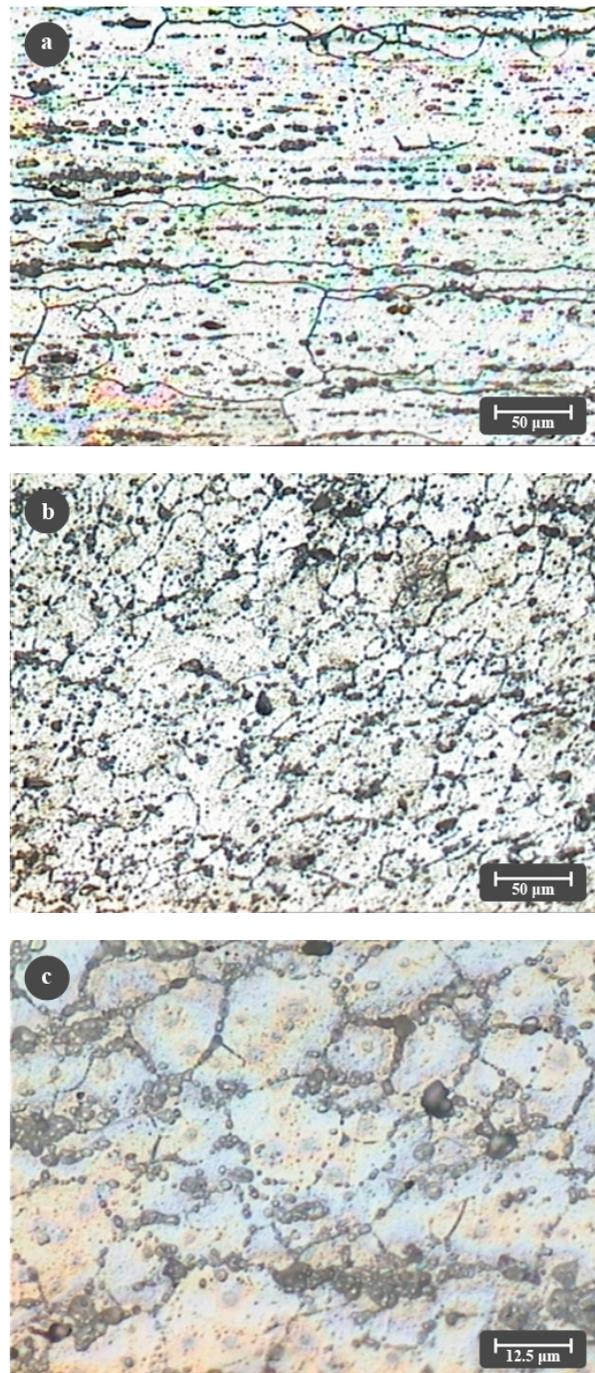
Fig 1. Microstructures of the weld nugget: a) parent alloy, ×200, b) weld zone, ×200 and c) weld zone, ×800; Etched by boiling HNO_3 (25%) solution.

cathode/anode area ratio in the galvanic study) and also identical couple electrodes from WZ and PA using a ZRA technique. The galvanic coupling tests were performed during 3600 s (data recorded every 1 s) and the reference electrode was SCE.

Results and Discussions

Morphological observations were carried out on the cross sections of weld nugget. The micrographs in Fig. 1 show the microstructures of parent alloy and weld zone. According to Fig. 1a, PA shows the elongated grain structure formed by mechanical working, which is identified as "bonding" structure. Furthermore, presence of metallurgical defects is dominant. Fig. 1b&c, also, exhibit the microstructures of WZ. Comparing Fig. 1b and Fig. 1b reveals WZ has equiaxed and more fine grains than PA due to dynamic recrystallization. In ×800 magnification (Fig. 1c), aggregation of the precipitated particles along the grain boundaries can be seen which not have polygonal shape in contrast with the parent alloy.

By metallographic observations, no distinct region as the heat affected zone (HAZ) can be observed, but the morphologies of PA and WZ are just separated by structural changing. Moreover the strip of thermo-mechanically affected zone (TMAZ), which is formed in the structure as the result of stirring during FSW, was not clearly identified. Since the region of TMAZ in comparison with the weld zone was very small and preparing an individual electrode from this area was impossible, weld zone and parent alloy were chosen as the working electrodes for electrochemical investigations.

Fig. 2a illustrates the results of potentiodynamic polarization of PA and WZ in 3.5% NaCl solution. It is evident that there is no significant difference between their polarization curves. The branches of anodic and cathodic curves are similar. Anodic branch of the polarization curve shows that the anodic dissolution is under activation control and the cathodic branch, up to -1100 mV, is under the control of oxygen diffusion and beyond this potential the cathodic reaction is under activation control of water reduction reaction. In order to differentiate the zero current potential (rest potential) between zones, the polarization curves are plotted in detail in Fig. 2b. The maximum difference between the rest potentials is about 20 mV. The average value of rest potential for WZ is -679 mV while the value for PA is almost -683 mV.

Based on the electrochemical reactions of aluminum and its alloys in neutral chloride containing environment, the following anodic reaction for anodic polarization of aluminum is proposed:

$$Al + 3H_2O \rightarrow Al(OH)_3 + 3H^+ + 3e^- \qquad (1)$$
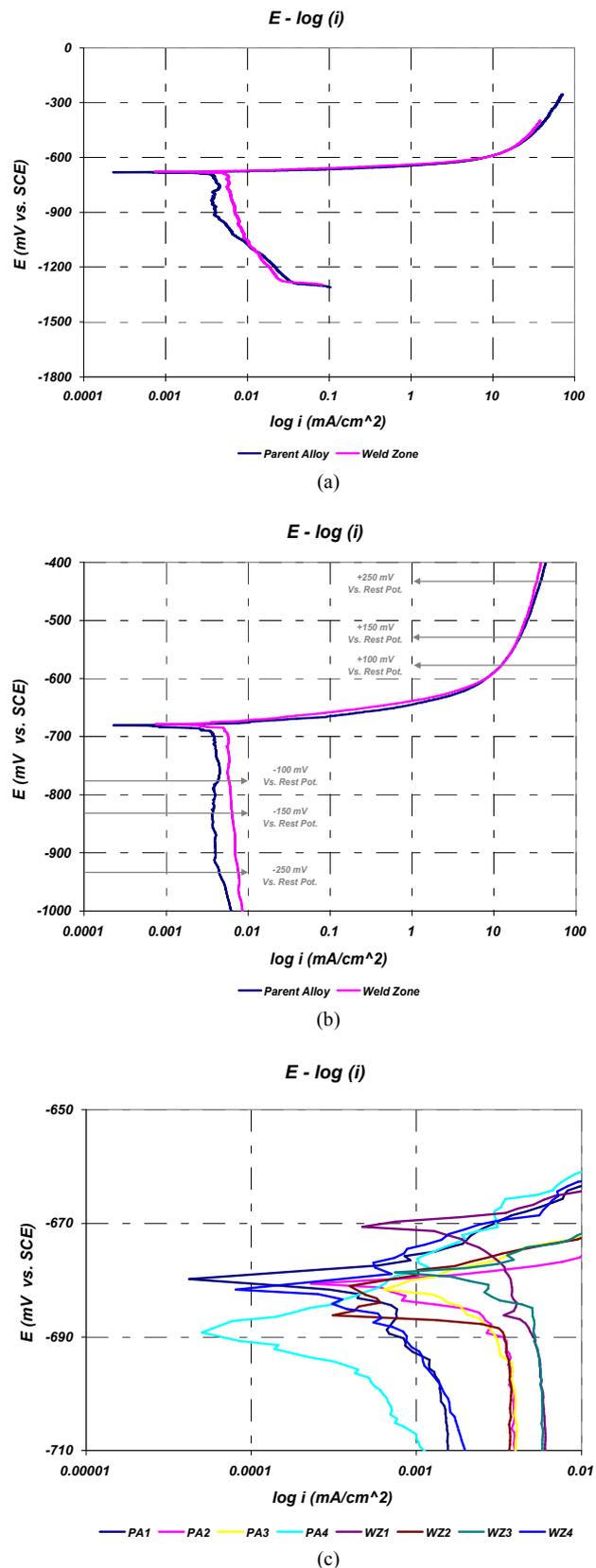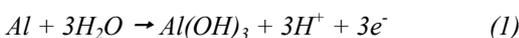
Fig 2. Potentiodynamic polarization curves in 3.5% NaCl solution at room temperature: a) parent alloy and weld zone, b) focused in order to estimate rest potential and c) the situation of applied potential in potentiostatic polarizations.

Since pitting potential of the alloy is coincident to the rest potential, formation of pit leads to the dissolution of aluminum according to the following reaction causing migration of chloride ions into the pit and formation of aluminum chloride inside the pit:

$$Al \rightarrow Al^{3+} + 3e^- \qquad (2)$$

$$Al^{+3} + 3Cl^- \rightarrow AlCl_3 \qquad (3)$$
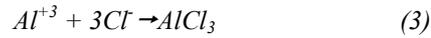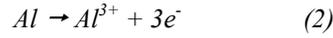
On the other hand, the following electrochemical
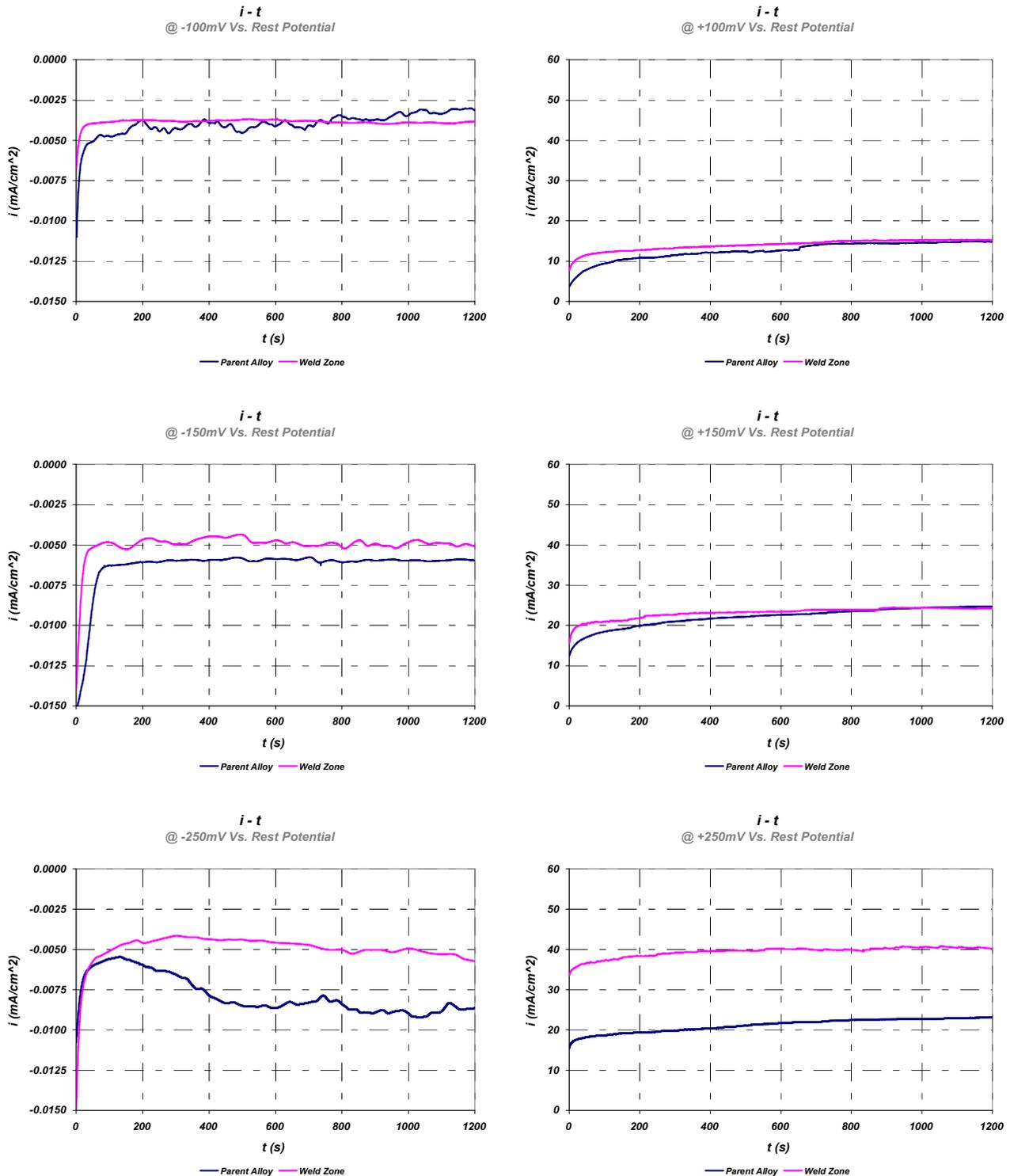
Fig 3. Potentiostatic polarization curves in 3.5% NaCl solution at room temperature for parent alloy and weld zone at different applied potentials versus rest potential.

reaction is proposed for the cathodic polarization of aluminum:

$$O_2 + 2H_2O + 4e^- \rightarrow 4OH^- \qquad (4)$$

$$2H_2O + 2e^- \rightarrow 2OH^- + H_2 \qquad (5)$$
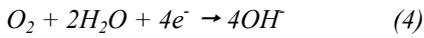
Employing FSW technique to join two pieces of metal or an alloy instead of using other techniques, based on filling the gap between two pieces by filler metal, has the advantage of less possibility of galvanic corrosion occurrence in weld area as a result of corrosion potential difference caused by chemical composition difference between weld and parent zones. Table 1 shows the four corrosion potential measurements extracted form the zero current density point of E–*log* curves. The mean values of corrosion potential difference between two zones are less than 5 mV which is very negligible. This means their difference, acting as the driving force for galvanic corrosion occurrence, is slight.

In order to magnify any difference in anodic and cathodic polarization of WZ and PA, several potentials were selected in anodic and cathodic branches of their polarization curves which are illustrated in Fig. 2c. Three anodic potentials of 100, 150 and 250 mV, above corrosion potential, and three potentials of -100, -150 and -250 mV respect to the corrosion potential were chosen. Fig. 3 illustrates the results of potentiostatic polarization at different applied potentials. It is evident the resoling current density at each applied potential is very similar for the PA and WZ. The major difference between these i-t curves obtained from potentiostatic polarization test, was observed at applied anodic potential of +250 mV respect to the corrosion potential. The current density associated to the WZ was almost twice of that for PA. This difference is also resulted from their potentiodynamic polarization curves which are shown in Fig. 2a.

Recording rest potential (corrosion potential) of two described electrodes for a period of one hour is illustrated in Fig. 4. No significant difference between their corrosion potential is observed and this is also expressed that it is a significant driving force for initiation of galvanic corrosion when two electrodes are connected to each other and immersed in a corrosion electrolyte such as 3.5% NaCl. The corrosion potential is varied around -700 mV for the measurement period. The variation of corrosion potential is almost smooth for WZ which is noisier for PA. This may be attributed to the higher degree of second phase particles that can act as initiation sites for metastable pits.

The possibility of galvanic corrosion occurrence was investigated using zero resistance ammetery techniques in order to measure the galvanic couple potential and galvanic couple current densities between couple electrodes. The couple electrodes were selected in two categories; identical electrodes which were the connection of two identical electrodes from weld zone, named WZ/WZ, and identical electrodes from parent alloy, named PA/PA. Another couple electrode set-up was selected from two nonidentical electrodes, one from weld zone and the other from parent alloy, which is named here as PA/WZ. All the galvanic measurements were carried out at room temperature and in 3.5% NaCl solution. The reason of choosing identical couple electrodes was to compare the measured current density of these couples and the current density which is measured from two nonidentical electrodes. Bearing in mind that theoretically there is no driving force for galvanic corrosion occurrence between two identical electrodes where two electrodes are completely identical from the morphological point of view and chemical composition. Any difference between the two electrodes due to chemical composition or morphology can cause a galvanic cell formation and leads to generation of current

Table 1. The values of rest potentials obtained from Tafel curves for different tests.

	$E_{Corr.}$ (mV)	
	Parent Alloy	**Weld Zone**
1st	-679.8	-670.6
2nd	-680.6	-686.1
3rd	-681.7	-678.6
4th	-689.2	-681.6
Ave.	-682.8	-679.2
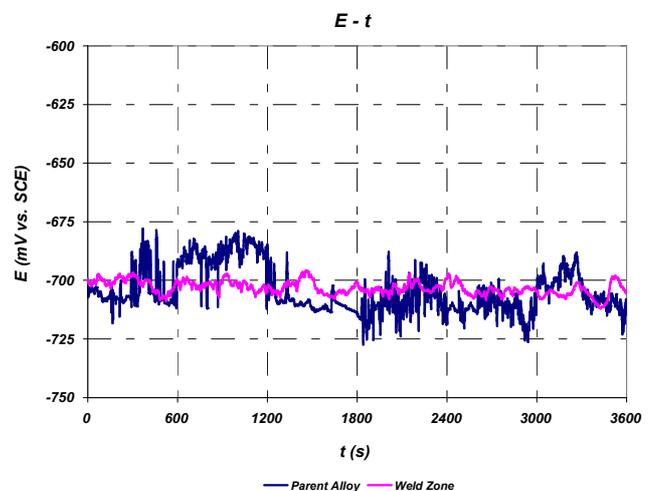
Fig 4. The curve of corrosion potential monitoring in 3.5% NaCl solution at room temperature for parent alloy and weld zone.
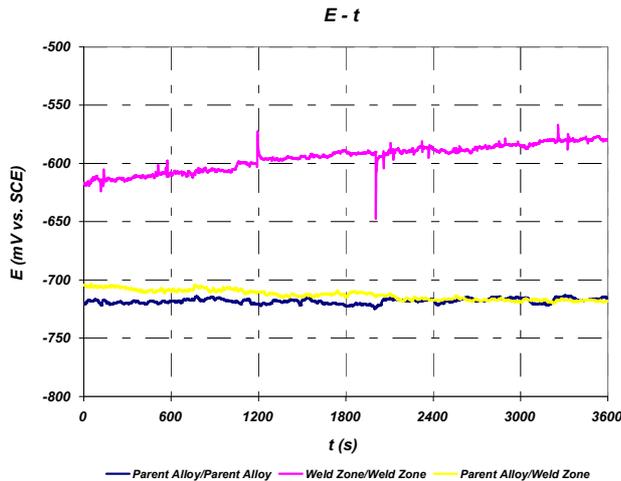
Fig 5. The variations of potential in galvanic coupling of parent alloy and weld zone electrodes for identical couple electrodes as well as nonidentical couple electrode.

Fig 6. The variations of current density in galvanic coupling of parent alloy and weld zone electrodes for identical couple electrodes as well as nonidentical couple electrode.

from the anode of the cell to the cathode.

Fig. 5 shows the results of couple potential variations with time for the mentioned three galvanic couples; two identical couples and the other nonidentical couple. The couple galvanic potential is the potential of intersection of the branche of cathodic current density of cathode from the polarization curve (E‑*log*i) with the anodic current density of the anode of the couple from its polarization curve (E‑*log*i). It is evident that the couple potential of nonidentical couple is very close to the identical couple electrode of PA/PA; while it has almost 100 mV different (more anodic) to the couple potential of identical couple of WZ/WZ.

Comparison of galvanic couple current density of the cells (Fig. 6) gives more information about the cell galvanic current. The galvanic current of the identical electrodes made from weld zone (WZ/WZ) is changing around zero for the course of one hour measurement, while the galvanic current of the other two identical electrodes made from parent alloy (PA/PA) has the magnitude of about 3 $\mu A.cm^{-2}$ during one hour measurement. The dissimilarity of these two electrodes is perhaps due to the difference in the dispersion of second phase particles that causes this negligible current density. On the other hand, a net current density of about

5.5 $\mu A.cm^{-2}$ is measured between two nonidentical electrodes, One selected from the WZ while the other from the PA, which is the result of difference between the morphology of two electrodes. Based on the very small difference between their corrosion potential (according to the Table 1), it is proposed that the PA acts as an anode of the cell while the WZ acts as the cathode. Long term immersion of the welded alloy in the solution causes knife corrosion in the parent alloy at the adjacent of the weld zone.

Table 2 shows the average values of the couple current density during one hour measurements of galvanic couples. It is evident that the measured current between two nonidentical couple electrodes (PA/WZ) is almost twice of the two identical couple electrodes between parent alloy (PA/PA).

Conclusion

• The results of morphological observation revealed there is no distinct heat affected zone (HAZ) and that the weld zone is just distinguished by structural changing from elongated grains, formed by mechanical working in parent alloy to recrystallized equiaxed grains.

• In the 6xxx series aluminum alloy jointed by friction stir welding technique, it was characterized the parent alloy and weld zone represent similar corrosion behavior. The potentidynamic polarization diagrams for both of them had the same progression in either chatodic or anodic directions. Furthermore, the results of potentiostatic polarizations tests have confirmed the fact.

• The E-*log*i diagrams showed that the anodic reactions were strongly controlled by activation energy mechanism so that the low increasing (~100 mV) of the potential results in very drastic rising of current density (up to 10^5 times). After that, the reactions were controlled by

Table 2. The values of rest potentials obtained from Tafel curves for different tests.

	E_G (mV)	$|i_G|$ ($\mu A.cm^{-2}$)
Parent Alloy/Parent Alloy	-718.2	2.286
Weld Zone/Weld Zone	-595.0	0.800
Parent Alloy/Weld Zone	-712.9	3.513

diffusive controlled mechanism as a result of intensive anodic reactions.

- The galvanic couple measurements showed that the current density in parent alloy/weld zone was approximately twice parent alloy/parent alloy and five times weld zone/weld zone indicating the occurrence of galvanic corrosion between weld zone and parent alloy. But the reason of why the galvanic potential of weld zone/weld zone was nobler, about 120 mV, could not be founded.

Acknowledgement

References

[1] A.B.M. Mujibur Rahman, S. Kumar, A.R. Gerson; Corros. Sci. 49 (2007) 4339-4351.

[2] E. Blasco-Tamarit, A. Igual-Munoz, J. García Antón, D. García-García; Corros. Sci. 48 (2006) 863-886.

[3] O. Hatamleh, P. M. Singh, H. Garmestani; Corros. Sci. 51 (2009) 135-143.

[4] C. Liu, D.L. Chen, S. Bhole, X. Cao, M. Jahazi; Mater. Charact. xx (2008) xxx-xxx.

[5] J. Corral, E. A. Trillo, Ying Li, L. E. Murr; J. Mater. Sci. Lett. 19 (2000) 2117-2122.

[6] C.S. Paglia, R.G. Buchhei; Scr. Mater. 58 (2008) 383-387.

[7] S. Lim, S. Kim, Ch.G. Lee, S. Kim; Metall. Mater. Trans. A 36A (2005) 1977-1980.

[8] P. B. Srinivasan, W. Dietze, R. Zettler, J.F. dos Santos, V. Sivan; Mater. Sci. Eng., A 392 (2005) 292-300.

[9] M. Jariyaboon, A.J. Davenport, R. Ambat, B.J. Connolly, S.W. Williams, D.A. Price; Corros. Sci. 49 (2007) 877-909.

[10] C.S. Paglia, R.G. Buchheit; Mater. Sci. Eng., A 492 (2008) 250-254.

[11] Stefano Maggiolino, Chiara Schmid; J. Mater. Process. Technol. 197 (2008) 237-240.